Published in final edited form as:
J Immunol. 2011 September 15; 187(6): 2885–2897. doi:10.4049/jimmunol.1100241.

Heterogeneous and tissue specific regulation of effector T cell responses by IFN-γ during *Plasmodium berghei* ANKA infection[1]

Ana Villegas-Mendez[*], **J. Brian de Souza**[*,†], **Linda Murungi**[*,‡], **Julius C. R. Hafalla**[*], **Tovah N. Shaw**[*], **Rachel Greig**[*,§], **Eleanor M. Riley**[*], and **Kevin N. Couper**[2,*]

[*]Department of Immunology and Infection, Faculty of Infectious and Tropical Diseases, London School of Hygiene and Tropical Medicine, Keppel Street, London WC1E 7HT, UK.

[†]Department of Immunology and Molecular Pathology, University College London Medical School, 46 Cleveland Street, London, W1T 4JF, UK

Abstract

IFN-γ and T cells are both required for the development of experimental cerebral malaria during *P. berghei* ANKA infection. Surprisingly, however, the role of IFN-γ in shaping the effector $CD4^+$ and $CD8^+$ T cell response during this infection has not been examined in detail. To address this, we have compared the effector T cell responses in wild-type and IFN- $\gamma^{-/-}$ mice during *P. berghei* ANKA infection. The expansion of splenic $CD4^+$ and $CD8^+$ T cells during *P. berghei* ANKA infection was unaffected by the absence of IFN-γ but the contraction phase of the T cell response was significantly attenuated. Splenic T cell activation and effector function were essentially normal in IFN- $\gamma^{-/-}$ mice, however, the migration to, and accumulation of, effector $CD4^+$ and $CD8^+$ T cells in the lung, liver and brain was altered in IFN- γ−/− mice. Interestingly, activation and accumulation of T cells in various non-lymphoid organs was differently affected by lack of IFN-γ, suggesting that IFN- γ influences T cell effector function to varying levels in different anatomical locations. Importantly, control of splenic T cell numbers during *P. berghei* ANKA infection depended upon active IFN- γ-dependent environmental signals – leading to T cell apoptosis - rather than upon intrinsic alterations in T cell programming. This is the first study to fully investigate the role of IFN- γ in modulating T cell function during *P. berghei* ANKA infection and reveals that IFN-γ is required for efficient contraction of the pool of activated T cells.

Introduction

Plasmodium berghei ANKA infection in susceptible strains of mice leads to the development of experimental cerebral malaria (ECM), a neuropathy that shares many similarities with human cerebral malaria (reviewed 1, 2). The pathogenesis of the terminal stages of ECM is still poorly defined, but it is clear that the prototypic type-1 cytokine IFN-γ plays a pivotal role in the development of cerebral pathology (3-5). Thus, IFN- γ–deficient (IFN-$\gamma^{-/-}$) and IFN- γ receptor (IFN- γR)-deficient (IFN-$\gamma R^{-/-}$) mice on susceptible backgrounds, including C57BL/6, fail to develop ECM (3, 4). Notably, high

[1]Grant support: This study was supported by the Wellcome Trust (Grant ref: 074538) and the UK Biotechnology and Biological Sciences Research Council (Grant ref: 041611). KNC holds a Career Development Fellowship from the UK Medical Research Council (Grant ref: G0900487).

[2]Corresponding author: kevin.couper@lshtm.ac.uk Tel: (44) 207 927 2690 Fax: (44) 207 927 2807 .
[‡]Present address: KEMRI Centre for Geographic Medicine Research, Coast, P.O. Box 230-80108, Kilifi, Kenya
[§]Present address: Breakthrough Breast Cancer, Weston House, 246 High Holborn, London WC1V 7EX

levels of circulating IFN- γ and upregulation of IFN-responsive genes are also correlated with development of cerebral malaria (CM) in humans (reviewed in 6).

It is currently unclear if the resistance of IFN-γR$^{-/-}$ mice to ECM is primarily due to alterations in innate cell or T cell activity, or a combination of both. Both macrophage accumulation within the brain and macrophage function (TNF secretion) are reduced in *P. berghei* ANKA-infected IFN- γR$^{-/-}$ mice compared to infected wild-type mice (3), suggesting that IFN-γ-responsive macrophages may contribute to the aetiology of ECM. On the other hand, IFN-γ regulates the expression of CCR2, CXCR3, ICAM-1, VCAM-1 and LFA-1 (3, 7) and the production of CCL5 (RANTES), CXCL10 (IP-10), MIG (CXCL9) in the brain during *P. berghei* ANKA infection (4, 7) suggesting that IFN-γ may contribute to ECM by directing the recruitment of T cells to the brain. In support of this hypothesis, CD8$^+$ T cells, primed in the spleen during *P. berghei* ANKA infection via cross-presentation of antigen by classical lymphoid dendritic cells (8-10), have been shown to migrate to the brain via CXCR3-CXCL10 (IP-10), MIG (CXCL9) and CCR5-CCL5 (RANTES) dependent pathways (4, 7, 11-13). T cell migration to the brain is thus reduced in IFN- γ(R) deficient mice (refs) (7). Since migration of CD8$^+$ T cells to the brain is believed to be a key process in the development of ECM (reviewed 14), through modulating parasite tissue biomass and/or causing direct endothelial cell damage (15-18), these data suggest that alterations in chemokine pathways and resultant attenuated migration of CD8$^+$ T cells is a major reason for the resistance of IFN-γ$^{-/-}$ and IFN-γR$^{-/-}$ mice to ECM.

There is, however, significant evidence from other models that IFN-γ may directly control the activation and expansion of T cells: IFN-γ drives STAT1-dependent expression of T-bet in CD4$^+$ T cells, which is the initial step in the differentiation of Th1 cells (19, 20). IFN- γR signalling is also required to repress IL-4 production by Th1 cells during recall responses (21) and IFN- γ modulates microglial activation within the brain during experimental autoimmune encephalitis (EAE), controlling both Th1 and Th2 cell activation (22). Consequently, in the absence of direct IFN- γR signalling, Th1 and CD8$^+$ T cell responses are impaired (23-25). Thus, reduced accumulation of T cells in the brains of IFN- γ$^{-/-}$ mice during *P. berghei* ANKA infection may not be solely due to altered chemotactic signals, but may also be a consequence of impaired T cell activation or differentiation.

In addition to its immunostimulatory effects, IFN- γ may also suppress T cell hyperactivity by limiting CD4$^+$ and CD8$^+$ T cell accumulation or expansion through the induction of apoptosis (26-33) and by deletion of Ag-presenting dendritic cells (34). Although few studies have examined in detail the apoptotic pathways regulated by IFN-γ, it has been shown that intrinsic (mitochondrial) and extrinsic (TRAIL, DR5 and TNFR1) pathways of apoptosis are induced in CD4$^+$ T cells by IFN- γ during BCG infection (28) and IFN- γ promotes caspase-8 dependent activation-induced cell death (AICD) of CD4+ T cells *in vitro* following TCR stimulation (32). Interestingly, it has been suggested that IFN- γ-dependent apoptosis can occur by paracrine signalling without expression of IFN- γR on T cells (29, 33), and through autocrine cell-specific IFN- γ signalling (30). With relevance to malaria infection, Ag-specific (but not non-specific) T cell apoptosis has been described during *P. berghei* ANKA, *P. yoelii* and *P. chabaudi* AS infections (27, 35, 36). Loss of splenic Ag-specific CD4$^+$ T cells was reduced when cells were adoptively transferred into mice treated with anti-IFN- γ (31), suggesting that IFN- γ was responsible for apoptosis. Importantly, however, the contribution of modified migratory behaviour following treatment with anti-IFN- γ leading to changes in splenic T cell numbers was not addressed. In separate studies, Ag-specific T cell apoptosis has been shown to occur during malaria infection through distinct death receptor- and bax-dependent pathways (37).

Europe PMC Funders Author Manuscripts

In this study we have compared the T cell response in WT and IFN- $\gamma^{-/-}$ mice during *P. berghei* ANKA infection to characterise the alterations in T cell-mediated immune functions that underlie the resistance of IFN-$\gamma^{-/-}$ mice to ECM. Our results show that IFN- γ is not required for activation of splenic $CD4^+$ and $CD8^+$ T cells during infection but that it is essential for contraction of the splenic effector T cell population through induction of apoptosis. Moreover, we demonstrate that IFN- γ - directs tissue specific migration of $CD8^+$ T cells and $CD4^+$ T cell, but not $CD8^+$ T cell, activation and effector function within peripheral organs. Importantly, we show that persistence of effector T cells in the spleen in IFN- $\gamma^{-/-}$ mice is due to the absence of active environmental cues during the precise period of ECM development, rather than due to intrinsic differences in T cell programming imprinted during the early stages of infection.

Materials and Methods

Animals and parasites

C57BL/6 ($CD45.2^+$), C57BL/6 IFN-γ knock out (IFN-$\gamma^{-/-}$) and C57BL/6 Ly5.1 ($CD45.1^+$) mice were bred in-house or purchased from Harlan, Oxford, UK and maintained in individually ventilated cages. Male and female mice were used in separate experiments, and were between 6 and 9 weeks of age. Cryopreserved *P. berghei* ANKA (*Pb* ANKA) parasites were thawed and passaged once *in vivo* in C57BL/6 mice before being used to infect experimental animals. Experimental mice were infected intravenously (i.v.) with 10^4 parasitised red blood cells (pRBC). Parasitaemia was monitored daily by microscopic examination of Giemsa (BDH)-stained thin blood smears. The severity of ECM was determined using a grading system: 1=no signs; 2=ruffled fur/and or abnormal posture; 3=lethargy; 4=reduced responsiveness to stimulation and/or ataxia and/or respiratory distress/hyperventilation; 5= prostration and/or paralysis and/or convulsions. All animals were euthanized when observed at stage 4 or 5.

Tissue processing and flow cytometry

Single cell suspensions of spleen, liver and lung were prepared by homogenising tissues through a 70 μm cell strainer (BD Falcon). Brains were cut into small pieces, aspirated through a 5ml syringe and incubated in HBSS containing 10% FCS with collagenase/dispase (2mg/ml) (Sigma) for 45 mins at room temperature. The brain suspension was then homogenised through a 70μm cell strainer, overlayed on a 30% percoll gradient and centrifuged at 1800g for 10 minutes. The mononuclear cell pellet was collected. Red blood cells were lysed in all samples by the addition of 1% lysing buffer (BD Bioscience). Absolute cell numbers were calculated using a haemocytometer and live/dead cell differentiation was performed using Trypan Blue (Sigma). To examine T cell activation 1×10^6 cells per sample were stained with anti-CD4 (RM4.5), anti-CD8 (53-6-7), anti-CD11a (M17/4), anti-CD25 (PC61), anti-CD27 (LG.7F9), anti-CD44 (1M7), anti-CD62L (MEL-14), anti-CD69 (H1-2F3), anti-CD71 (R17217), anti-CXCR3 (CXCR3-173), anti CD45.1 (A20), anti-CD45.2 (104), anti-CD49D (R1-2), anti-PD-1 (RMP1-30), Annexin V and 7-AAD. Intracellular staining for Granzyme B (16G6), anti-CTLA-4 (UC10-4B9) and anti-Ki67 (B56) was performed by permeabilising cells with 0.1% Saponin/PBS. To quantify macrophage/monocyte numbers, 1×10^6 cells per sample were stained with anti-F4-80 (BM8), anti-CD11b (M1/70) and anti-CD3 (17A2), to exclude lymphocytes. To assess ex vivo cytokine production, 1×10^6 live cells were incubated with PMA (200ng/ml) and ionomycin (1μg/ml) in the presence of Brefeldin A (E-Bioscience) for 5hrs at 37°C 5% CO2. The cells were washed and intracellular staining with anti-mouse IFN-γ (XMG1.2) and anti-mouse TNF (MP6-XT22) was performed as above. All antibodies were obtained from eBioscience or BD-Bioscience. Flow cytometric acquisition was performed using a

FACSCalibur or LSR-II (both BD Immunocytometry Systems, USA) and all analysis was performed using Flowjo software (Treestar Inc., OR, USA).

$CD4^+$ and $CD8^+$ T cell isolation

$TCR\beta^+$ or $CD4^+$ and $CD8^+$ T lymphocytes were positively selected using anti-mouse conjugated midiMACS beads (Miltenyi Biotec) according to the manufacturer's instructions. In some experiments, purified $CD4^+$ and $CD8^+$ T cells were snap frozen in liquid nitrogen and stored at −80°C for real time PCR analysis. In separate experiments, 5-7 $\times 10^6$ purified T cells were adoptively transferred into recipient mice on day 5 after infection with *P. berghei* ANKA. The purity of positively selected T cell populations was assessed by flow cytometry prior to adoptive transfer or PCR analysis and was typically found to be greater than 90%.

Real Time PCR

RNA isolation from purified $CD4^+$ and $CD8^+$ T cells was performed using RNAeasy isolation kits according to the manufacturer's instructions (Qiagen). Isolated RNA was DNAse treated to remove genomic DNA prior to synthesis of cDNA. cDNA expression for each sample was standardised using the housekeeping genes GAPDH or β-actin. Data are presented as fold change ($\log_{10}$) in gene expression in infected IFN-$\gamma^{-/-}$ cells/tissues relative to infected WT cells/tissues. Results for each gene were calculated using the formula $2^{\wedge}$(Average normalised WT − normalised IFN-$\gamma^{-/-}$). Validated gene expression assays for T-bet, RORγT, GATA-3, IL-4, IL-17, perforin, Bcl-2, BAD, BAX, BIM, CXCl9, CXCL10, RANTES, VCAM-1 and ICAM-1 were purchased from ABI Biosystems (Warrington, UK). PCR Cycling (Taqman, ABI 7500 fast RT-PCR) conditions were: 50 °C for 2 min, 95 °C for 10 min followed by 40 cycles of 15 sec at 95 °C completed with 1 min at 60 °C.

Statistical analysis

Statistical significance was determined using two tailed Student's t test, unless otherwise stated, with $P < 0.05$ taken as indicating a significant difference.

Results

IFN-γR is heterogeneously expressed on naive and effector T cells in different organs during *P. berghei* ANKA infection

Consistent with previous studies, WT C57BL/6 mice were exquisitely susceptible to the development of ECM during *P. berghei* ANKA infection. In contrast, IFN-$\gamma^{-/-}$ deficient mice were completely resistant to ECM, even though peripheral parasitaemia was comparable in WT and IFN-$\gamma^{-/-}$ mice throughout the course of infection (Supplementary Figure 1). To determine whether T cells may be directly controlled by IFN-γ during *P. berghei* ANKA infection, contributing to the development of ECM, we evaluated the T cell-intrinsic expression of the IFN-γR on naive and activated ($CD44^+$) $CD4^+$ and $CD8^+$ T cells in WT mice in various tissues during the course of infection. We observed that the frequency of $CD4^+$ and $CD8^+$ T cells expressing the IFN-γR increases during infection in the spleen, lung, liver and brain (Figure 1 and Supplementary Figure 2). In naive mice, IFN-γR was expressed predominantly by effector ($CD44^+$) CD4 and CD8+ T cells in all organs (Figure 1). In contrast, during malaria infection, IFN-γR was heterogeneously expressed on both naïve and effector $CD4^+$ and $CD8^+$ T cells and the frequency of IFN-γR^+ cells (and the MFI of IFN-γR expression) varied significantly between the different tissues (Figure 1).

IFN-γ is not required for the activation of splenic CD4+ and CD8+ T cell populations during *P. berghei* ANKA infection

To investigate whether the T cell response differed between infected WT and IFN-$\gamma^{-/-}$ mice, we first examined the total numbers of splenic $CD4^+$ and $CD8^+$ T cells during the course of infection: the spleen is believed to be the primary site of immune priming during blood stage malaria infection (reviewed 38). Splenic $CD4^+$ and $CD8^+$ T cell numbers increased at a comparable rate, and plateaued at equivalent levels, in WT and IFN-$\gamma^{-/-}$ mice suggesting that the initial expansion phase of the T cell response was unimpaired in the absence of IFN-γ (Figure 2A). Indeed, splenic T cell proliferation, as measured by the frequencies of cells expressing Ki67, was comparable in WT and IFN-$\gamma^{-/-}$ mice (results not shown but provided for review). However, the subsequent contraction of splenic $CD4^+$ and $CD8^+$ T cell numbers, between days 5 and 7 post-infection, was markedly attenuated in IFN-$\gamma^{-/-}$ mice compared to WT mice (Figure 2A). Furthermore, in the absence of IFN- γ, expression of the early activation marker CD69 was significantly attenuated on both $CD4^+$ and $CD8^+$ T cells, this was most evident on day 5 post infection, and Granzyme B expression was reduced on day 7 in $CD4^+$ and $CD8^+$ T cells (Figure 2B, C). Additionally, reduced frequencies of splenic $CD4^+$ T cells (but not CD8+ T cells) expressed CTLA-4 on day 7 of infection in IFN-$\gamma^{-/-}$ mice (Supplementary Figure 3). Thus, these data suggest that there may be small defects in T cell function in the absence of IFN-γ. On the other hand, lack of IFN-γ led to only transient differences in expression of all other examined activation markers. Similar frequencies of $CD62L^{low}$, $CD44^+$, $CD25^+$, $CD27^{low}$, $CD11a^+$, $CD49D^+$ and PD-1^+ splenic T cells were observed in WT and IFN-$\gamma^{-/-}$ mice throughout the course of infection (Figure 2B, C; Supplementary Figure 3; CD49D results not shown) although, due to the failure of the T cell population to contract in IFN-$\gamma^{-/-}$ mice, total numbers of activated T cells were higher in these mice than in WT mice by day 7 post-infection.

IFN-γ fine tunes splenic T cell polarisation and effector function during *P. berghei* ANKA infection

TNF is a potent pro-inflammatory cytokine that is induced by IFN-γ and is associated with severe malarial disease (reviewed 38). Thus, we examined whether TNF production by $CD4^+$ and $CD8^+$ T cells was reduced in IFN-$\gamma^{-/-}$ mice (Figure 3). A large proportion (> 30%) of $CD4^+$ and $CD8^+$ T cells from both naïve WT and naïve IFN-$\gamma^{-/-}$ mice produced TNF-α after PMA/ionomycin restimulation. TNF responses were maintained throughout the course of infection and were broadly similar in WT and IFN-$\gamma^{-/-}$ mice; however, on day 5 of infection, the proportion of $CD4^+$ T cells expressing TNF and the mean fluorescence intensity of TNF expression in $CD4^+$ and $CD8^+$ T cells was significantly lower among IFN-$\gamma^{-/-}$ mice than among WT mice. These data imply that in the absence of IFN-γ, T cells have a slightly reduced capacity to produce TNF-α at a key stage of *P. berghei* ANKA infection.

As expected, IFN-γ production was completely abrogated in IFN-$\gamma^{-/-}$ CD4+ and CD8+ T cells whereas $CD4^+$ and $CD8^+$ T cells producing IFN-γ (alone or in combination with TNF) were observed in WT mice throughout the course of infection. Of note, the $CD8^+$ T cells with the highest levels (MFI) of TNF-α production also produced IFN-γ (Figure 3B).

Perhaps surprisingly, given that IFN-γ has been shown to be an inhibitor of both Th2 and Th17 lineages (39, 40), we did not detect intracellular IL-17A/F at any time in either $CD4^+$ or $CD8^+$ T cells from either WT or IFN-$\gamma^{-/-}$ mice (data not shown); we had expected that expression of Th2 and Th17-associated genes would be increased in $CD4^+$ T cells from infected IFN-$\gamma^{-/-}$ mice. Indeed, expression of GATA3, RORγT and IL-4 mRNA was significantly higher in infection-derived IFN-$\gamma^{-/-}$ $CD4^+$ T cells than in corresponding WT $CD4^+$ T cells (Figure 4A, B). Nevertheless, expression of IL-17A, T-bet and perforin mRNA was similar in WT and IFN-$\gamma^{-/-}$ $CD4^+$ T cells (Figure 4A, B). Similarly, IL-4 mRNA

expression was higher in $CD8^+$ T cells from IFN-$\gamma^{-/-}$ mice compared to WT mice throughout infection, and although T-bet expression was slightly increased in IFN-$\gamma^{-/-}$ CD8+ T cells isolated on day 7 of infection compared with corresponding WT cells, the expression of IL-17 and perforin did not differ (Figure 4C). Thus, in the absence of IFN-γ, there are subtle effects on polarisation of - and cytokine production by - splenic $CD4^+$ and $CD8^+$ T cells during *P. berghei* ANKA infection but there is no large-scale change in T cell phenotype that might explain the complete resistance to ECM among IFN-$\gamma^{-/-}$ mice.

IFN-γ regulates tissue-specific accumulation of T cells during *P. berghei* ANKA infection

We hypothesised that migration to peripheral tissues (rather than cell death) was the cause of reduced splenic T cell numbers in WT mice on day 7 of *P. berghei* ANKA infection and thus that splenic T cell numbers might be maintained in IFN-$\gamma^{-/-}$ mice due to their reduced migration. To test this, we enumerated $CD4^+$ and $CD8^+$ T cells in brain, lung and liver of infected WT and IFN-$\gamma^{-/-}$ mice. Consistent with previous studies (4), $CD8^+$ T cell numbers were significantly higher in the brains of WT mice than those of IFN-$\gamma^{-/-}$ mice on day 7 post-infection (Figure 5A), however the difference in total brain T cell numbers (approx. 5,000 $CD8^+$ T cells per brain) was insufficient to account for the marked loss of T cells in the spleen in WT mice (Figure 2B). Moreover, similar (or even higher) numbers of $CD4^+$ and $CD8^+$ T cells were observed in the livers and lungs of IFN-$\gamma^{-/-}$ mice than in WT mice on day 7 pi (Figure 5B, C). Thus, although T cell migration does differ between WT and IFN-$\gamma^{-/-}$ mice during *P. berghei* ANKA infection, it is unlikely that the loss of splenic T cells in WT mice is simply due to enhanced T cell migration to peripheral tissues.

To determine whether altered T cell migration and tissue accumulation in IFN-$\gamma^{-/-}$ mice was due to cell-intrinsic differences in chemokine receptor expression, we compared T cell expression of CXCR3 and CCR5 (which have been shown to promote T cell migration during *P. berghei* ANKA infection; 7, 11-13) in WT and IFN-$\gamma^{-/-}$ mice. Although alterations in chemokine and chemokine receptor expression have been reported in *P. berghei* ANKA-infected IFN-γ(R)$^{-/-}$ mice (4, 7), T cell-specific CXCR3 and CCR5 expression has not been reported. We observed that CXCR3 is constitutively expressed on hepatic $CD4^+$ T cells and its expression is not affected by *P. berghei* ANKA infection (Figure 5D) and that CCR5 is upregulated to a similar extent on WT and IFN-$\gamma^{-/-}$ hepatic $CD4^+$ T cells during infection. CXCR3 and CCR5 are both upregulated by infection on $CD4^+$ T cells in the spleen, brain and lung, but this upregulation is significantly attenuated in IFN-$\gamma^{-/-}$ mice compared to WT mice (Figure 5D, E). In contrast, CXCR3 expression on $CD8^+$ T cells was upregulated to the same extent in WT or IFN-$\gamma^{-/-}$ mice (in all organs) during infection (Figure 5F). Similarly, CCR5 expression was comparable on $CD8^+$ T cells in WT and IFN-$\gamma^{-/-}$ mice within the spleen, lung and liver; expression was, however, reduced in $CD8^+$ T cells within the brain of IFN-$\gamma^{-/-}$ mice (Figure 5G). These data suggest that differences in $CD8^+$ T cell migration in IFN-$\gamma^{-/-}$ mice are more likely to be due to differences in chemokine production within individual tissues than to differences in chemokine receptor expression on T cells. In support of this conclusion, we observed significantly reduced expression of CXCL9 (MIG) and CXCL10 (IP-10) in the brains of IFN-$\gamma^{-/-}$ mice compared with WT mice on day 7 of infection (Supplementary Figure 4).

IFN-γ controls the activation of $CD4^+$ T cells but not $CD8^+$ T cells within peripheral tissues during *P. berghei* ANKA infection

Although similar levels of splenic T cell activation were observed in infected WT and IFN-$\gamma^{-/-}$ mice, it remained possible that the activation status of T cells migrating to, and accumulating in, the tissues may differ between WT and IFN-$\gamma^{-/-}$ mice. Importantly, upregulation of IFNγR expression in peripheral non-lymphoid tissues in infected WT mice (Figure 1), suggested that IFN-γ may be particularly important in controlling T cell effector

function in peripheral tissues. As ECM and respiratory distress during *P. berghei* ANKA have been associated with T cell accumulation in brain and lung, respectively, we next compared expression of various activation/memory markers on $CD4^+$ and $CD8^+$ T cells responses within brain and lung of infected WT and IFN-$\gamma^{-/-}$ mice (Figure 6). Interestingly, a smaller proportion of the brain-infiltrating $CD4^+$ T cells expressed an activated phenotype, as measured by CD44 and CD62L expression, in IFN-$\gamma^{-/-}$ mice than in WT mice (Figure 6A), although - despite the observation that the IFN-γR is expressed to equivalent levels on $CD4^+$ T cells in the lung and brain (Figure 1) - the proportions of activated $CD4^+$ T cells in the lungs did not differ between WT and IFN-$\gamma^{-/-}$ mice. Moreover, a smaller proportion of brain infiltrating (but not lung infiltrating) $CD4^+$ T cells expressed CD71, CD11a, Ki67, but not GrB, in IFN-$\gamma^{-/-}$ mice than in WT mice. In contrast, fewer $CD4^+$ T cells within the lung and brain expressed CD49D in IFN-$\gamma^{-/-}$ mice. Unexpectedly, given the marked reduction in accumulation of $CD8^+$ T cells in the brain and lung in IFN-$\gamma^{-/-}$ mice (Figure 5), $CD8^+$ T cell activation in the brain and lung was essentially unimpaired in IFN-$\gamma^{-/-}$ mice (Figure 6B). These data suggest that, during *P. berghei* ANKA infection, $CD4^+$ T cells are much more dependent on IFN-γ for their activation within the brain than are $CD8^+$ T cells. Furthermore, as Ki67 expression was comparable on brain-accumulating $CD8^+$ T cells in WT and IFN-$\gamma^{-/-}$ mice (Figure 6), our results show that enhanced accumulation of $CD8^+$ T cells within the brain of WT mice is not due to increased local extra-lymphoid proliferation. The expression of ICAM-1 and VCAM-1 was also unimpaired in IFN-$\gamma^{-/-}$ mice (Supplementary Figure 4). Thus, combined, our results, also suggest that the VLA-4 and LFA-1 pathways do not dominantly control $CD8^+$ T cell accumulation within the brain during *P. berghei* ANKA infection.

A reduced proportion of brain- and lung-infiltrating $CD4^+$ T cells expressed the T cell inhibitory receptors CTLA-4 and PD-1 in IFN-$\gamma^{-/-}$ mice compared with WT mice on day 7 of infection (Supplementary Figure 3). Similarly, reduced proportions of brain and lung-infiltrating $CD8^+$ T cells expressed CTLA-4 in IFN-$\gamma^{-/-}$ mice compared with WT mice on day 7 of infection. In contrast, PD-1 expression by $CD8^+$ T cells was unaltered in the absence of IFN-γ (Supplementary Figure 3). These results indicate that defective $CD4^+$ T cell activation within the brain of IFN-$\gamma^{-/-}$ mice is unlikely due to increased CTLA-4 and PD-1 mediated suppression.

IFN-γ limits splenic T cell numbers during *P. berghei* ANKA infection by promoting apoptosis

Since the loss of splenic T cells in *P. berghei* ANKA-infected WT mice does not seem to be due to increased migration of T cells to peripheral tissues, and since IFN-γ is known to control the contraction phase of the effector response by directing T cell apoptosis (26-33), we compared the frequencies of late stage apoptotic/dead T cells, determined by co-staining with 7-AAD and AnnexinV, in spleens of WT and IFN-$\gamma^{-/-}$ mice. We observed no significant differences in apoptotic T cell frequencies between uninfected WT and IFN-$\gamma^{-/-}$ mice, indicating that survival of resting T cells is unaffected by presence or absence of IFN-γ (Figure 7A-C). The frequency of apoptotic $CD4^+$ T cells increased significantly in WT mice, but not IFN-$\gamma^{-/-}$ mice, during *P. berghei* ANKA infection (Figure 7A, B). Similarly, significantly increased frequencies of late stage apoptotic $CD8^+$ T cells were observed in infected WT mice compared with infected IFN-$\gamma^{-/-}$ mice and uninfected mice, although the frequencies of late stage apoptotic $CD8^+$ T cells was increased in infected IFN-$\gamma^{-/-}$ mice compared with uninfected controls (Figure 7A, C).

To determine whether reduced T cell apoptosis in IFN-$\gamma^{-/-}$ mice was due to modulation of the intrinsic pathway of apoptosis we examined, by real-time PCR, the expression of the anti-apoptotic regulator Bcl-2 and the pro-apoptotic molecules BAD, BAX and BIM (Figure 7 D, E) in purified populations of $CD4^+$ and $CD8^+$ T cells. When compared to cells from

WT mice, on day 5 of infection expression of Bcl-2 was increased in $CD4^+$ and $CD8^+$ T cells from IFN-$\gamma^{-/-}$ mice, suggesting that upregulation of Bcl-2 protects these cells from apoptosis. Levels of BAD and BAX expression were similar in WT and IFN-$\gamma^{-/-}$ $CD4^+$ and $CD8^+$ T cells throughout the course of infection (Figure 7D, E). Surprisingly, however, expression of BIM was increased in IFN-$\gamma^{-/-}$ derived $CD8^+$ T cells (but not $CD4^+$ T cells) on days 5 and 7 of infection (Figure 7E). Taken together, these data suggest that the loss of splenic effector T cells during the course of *P. berghei* ANKA infection in WT mice is due to IFN-γ–mediated apoptosis: increased Bcl-2 expression may prevent apoptosis in IFN-$\gamma^{-/-}$ mice but apoptosis in WT mice is unlikely to proceed solely through the classical intrinsic pathway.

IFN-$\gamma^{-/-}$ T cells are lost from the spleen at a comparable rate and magnitude to WT T cells when placed in an IFN-γ sufficient environment

Our data suggest that, despite marked differences in their susceptibility to T cell-dependent immunopathology, the splenic effector T cell response is broadly similar in *P. berghei* ANKA infected WT and IFN-$\gamma^{-/-}$ mice with the only substantial difference being the increased resistance to apoptosis of T cells from IFN-$\gamma^{-/-}$ mice. To determine whether T cells maturing in the absence of IFN-γ are intrinsically resistant to apoptosis, or whether their resistance is simply due to the lack of circulating IFN-γ, we purified $CD4^+$ and $CD8^+$ T cells from WT and IFN-$\gamma^{-/-}$ mice on day 5 of *P. berghei* ANKA infection, transferred them into congenic ($CD45.1^+$), infected (day 5; i.e. at the peak of T cell expansion and prior to onset of apoptosis in WT mice) or uninfected, WT mice and determined their recovery 2 days later (i.e. day 7 of infection; peak of apoptosis in WT mice) (Figure 8). Representative dot plots showing the recovery of host ($CD45.2^-$) and donor ($CD45.2^+$) $CD4^+$ T cells in the spleen are shown in Figure 8A. As expected, significantly fewer donor $CD4^+$ T and $CD8^+$ T cells were recovered from spleens of infected recipient mice than from spleens of uninfected recipient mice (Figure 8B,C). This was associated with increased recovery of donor cells from the lungs in infected mice (Figure 8D, E), indicating preferential migration of donor T cells to peripheral tissues rather than the spleen during *P. berghei* ANKA infection. However, the increased accumulation of donor cells in non-lymphoid tissues in infected recipients was insufficient to account for the reduced recovery of donor cells in the spleen, strongly suggesting that apoptosis rather than cellular migration controlled donor cell recovery from the spleen. Importantly, $CD4^+$ T cells from IFN-$\gamma^{-/-}$ mice disappeared at the same rate as $CD4^+$ T cells from WT mice once transferred into an IFN-γ replete host. On the other hand, $CD8^+$ T cells from IFN-$\gamma^{-/-}$ donors survived better in both infected and uninfected recipients, than did $CD8^+$ T cells from WT donors (Figure 8C). Together, these data further indicate that effector $CD4^+$ T cells from WT and IFN-$\gamma^{-/-}$ mice are not intrinsically different and behave equivalently when placed in comparable (i.e. IFN-γ replete) environments. Although IFN-$\gamma^{-/-}$ splenic $CD8^+$ T cells seem slightly more resilient than WT $CD8^+$ T cells, they still succumb to IFN-γ-dependent signals during infection.

Contraction of the splenic T cell response in WT mice is an active process mediated on or after day 5 of infection

Our data strongly suggest that differences in maintenance of splenic T cell populations in *P. berghei* ANKA-infected WT and IFN-$\gamma^{-/-}$ mice are due to differences in an active process of cell survival and/or apoptosis beginning on or after day 5 of infection and mediated by extrinsic (environmental) signals. To test this hypothesis, we purified splenic $CD4^+$ and $CD8^+$ T cells from WT C57/BL6 $CD45.1^+$ congenic mice on day 5 of *P. berghei* ANKA infection and adoptively transferred them into infected (day 5 of *P. berghei* ANKA infection) and uninfected, WT and IFN-$\gamma^{-/-}$, $CD45.2^+$ mice. The survival of $CD45.1^+$ donor cells in spleen, lung and brain of infected and uninfected recipient mice was assessed two days after transfer, at the stage when WT mice developed ECM (Figure 9). Representative

dot plots showing the recovery of donor ($CD45.1^+$) and host ($CD45.1^-$) $CD4^+$ T cells from the spleen are shown in Figure 9A. In clear support of the hypothesis, more donor $CD4^+$ and $CD8^+$ T cells were recovered from spleens of infected IFN-$\gamma^{-/-}$ mice than from those of WT mice (Figure 9B, C); indeed, donor cell numbers in spleens of infected IFN-$\gamma^{-/-}$ mice were comparable to those in uninfected mice. Since identical cells were transferred into infected WT and IFN-$\gamma^{-/-}$ hosts, it is evident that loss of splenic T cells in WT mice is an active process, mediated by extrinsic IFN-γ after day 5 of infection. Importantly, the lower recovery of donor T cells from spleens of WT infected mice was not due to increased T cell migration to peripheral tissues as no donor cells were recovered from the brain (data not shown) and equivalent numbers of donor $CD4^+$ and $CD8^+$ T cells were found in the lungs of infected WT and IFN-$\gamma^{-/-}$ recipients (Figure 9D, E). Thus active, non-autocrine IFN-γ-dependent signals control splenic $CD4^+$ and $CD8^+$ T cell survival during *P. berghei* ANKA infection.

Discussion

We have performed a detailed comparison of the effector T cell response in WT and IFN-$\gamma^{-/-}$ mice infected with *P. berghei* ANKA to examine the extent to which cell-intrinsic differences in T cell function determine the resistance of IFN-$\gamma^{-/-}$ mice to ECM. We have found that $CD8^+$ T cell activation, which is an essential precursor of ECM development (reviewed 14), occurs entirely independently of IFN-γ signaling. However, lack of IFN-γ significantly reduced cerebral migration, or accumulation, of $CD8^+$ T cells; instead, in the absence of IFN-γ, $CD8^+$ T cells accumulated in other organs (such as the lung). Impaired accumulation of $CD8^+$ T cells within the brain of IFN-$\gamma^{-/-}$ mice was not due to attenuated *in situ* local proliferation. Although it has previously been suggested that IFN-γ upregulates CCR5- and CXCR3-dependent $CD8^+$ T cell migration pathways during malaria infection (4, 7), we have found that CXCR3 and CCR5 expression by $CD8^+$ T cells is unaffected (spleen, lung) or only marginally affected (brain) by lack of IFN-γ. Thus, our results suggest that CXCR3- and CCR5-dependent $CD8^+$ T cell migration to the lung and brain during *P. berghei* ANKA infection is unlikely to be controlled primarily at the level of chemokine receptor expression and is more likely dependent on the level of chemokine production within a particular tissue. If so, then IFN-γ may be an important inducer of chemokine expression in the brain, a supposition that is well supported by our data, which is consistent with published results (7), showing that production of IP-10 and MIG in the brain is abrogated in IFN-$\gamma^{-/-}$ mice. In contrast, as VLA-4 and LFA-1 expression by $CD8^+$ T cells was unimpaired in IFN-$\gamma^{-/-}$ mice, and the expression of ICAM-1 and VCAM-1 within the brain was comparable in WT and IFN-$\gamma^{-/-}$ mice during infection, our results strongly suggest that dysregulation of these adhesion pathways does not contribute to impaired accumulation of $CD8^+$ T cells within the brain of IFN-$\gamma^{-/-}$ mice (on C57BL/6 background) during *P. berghei* ANKA infection. The reason for the differences in our results compared with Van den Steen *et al* (7), who observed lower expression of ICAM-1 and VCAM-1 in the brains of IFN-$\gamma^{-/-}$ mice (DBA/2 and BALB/c backgrounds), is potentially due to the genetic background of the IFN-$\gamma^{-/-}$ mice used in the two studies. Indeed, in the study by Van den Steen et al (7), the fold change in expression of ICAM-1 and VCAM-1 within the brain of WT and IFN-$\gamma^{-/-}$ mice varied between BALB/c and DBA-2 mice.

Interestingly, IFN-γ seems to play a somewhat different role in regulating $CD4^+$ T cell responses to *P. berghei* ANKA infection. Despite lower expression of CCR5 and CXCR3, $CD4^+$ T cell accumulation in the brain and lung was unimpaired in *P. berghei* ANKA-infected IFN-$\gamma^{-/-}$ mice, consistent with findings in IFN-$\gamma R^{-/-}$ mice (4). This is even though fewer brain-derived $CD4^+$ T cells expressed the proliferative marker Ki67 in IFN-$\gamma^{-/-}$ mice, suggesting that IFN-γ may influence (effector or effector-memory) $CD4^+$ T cell proliferation within the brain during malaria infection. Thus, it is possible that $CD4^+$ T cells

may exit the brain and re circulate or the cells may die in situ in IFN-γ competent mice. On the other hand, the proportion of brain localised $CD4^+$ T cells with a highly activated phenotype was significantly reduced in IFN-$\gamma^{-/-}$ mice compared with WT mice. Therefore, in contrast to what we saw for $CD8^+$ T cells, $CD4^+$ T cell migration to and/or accumulation in peripheral tissues during *P. berghei* ANKA is controlled by IFN-γ independent processes but IFN-γ is essential for $CD4^+$ T cells to become fully activated. This raises the possibility that $CD4^+$ IFN-γ^+ T cells may modify the cerebral environment, promoting $CD8^+$ T cell migration and accumulation, which in an interdependent relationship may augment parasite biomass (15-17). In support of this, we have shown that adoptive transfer of infection-derived, IFN-γ–competent $CD4^+$ T cells into IFN-$\gamma^{-/-}$ mice increases $CD8^+$ T cell accumulation within the brain and induces ECM (manuscript in preparation) in an IFN-γ dependent manner. IFN-γ may modulate the function of tissue-resident cells, such as astrocytes or endothelial cells (22, 41), or modulate the accumulation of other infiltrating cells such as macrophages (results not shown but provided for review and reference 3).

In addition to its effects on T cell activation and migration, IFN-γ also regulates T cell survival in the spleen during *P. berghei* ANKA infection. The contraction phase of the effector T cell response was markedly attenuated in IFN-$\gamma^{-/-}$ mice, such that by day 7 of infection spleens of IFN-$\gamma^{-/-}$ mice contained two to three fold more T cells than did spleens of WT mice. Nonetheless, as peripheral parasitaemia was similar in WT and IFN-$\gamma^{-/-}$ mice, this stronger T cell response does not seem to translate into better parasite control and thus the resistance to ECM of IFN-$\gamma^{-/-}$ mice cannot be simply be due to lower parasite burdens (as seems to be the case in IP-$10^{-/-}$ mice; 43). Thus, we postulate that IFN-$\gamma^{-/-}$ mice are resistant to ECM due to lessened inflammation within the brain and resultant reduced local tissue-parasite accumulation and vascular haemorrhage. In support of this, brain parasite biomass is, known to be lower in IFN-$\gamma^{-/-}$ mice (16, 17). Our data suggest that IFN-γ promotes contraction of the effector T cell pool by inducing apoptosis, confirming earlier reports that IFN-γ induces apoptosis of malaria-specific $CD4^+$ T cells (31). Nevertheless, we have extended the analysis of the role played by IFN-γ to demonstrate that IFN-$\gamma^{-/-}$ T cells are fully susceptible to apoptosis when transferred into an IFN-γ sufficient environment, and that WT $CD4^+$ T cells are resistant to apoptosis when transferred to an IFN-γ deficient environment. In other words, extrinsic IFN-γ-signalling mediates apoptosis of T cells in infected mice, irrespective of whether the T cell itself can secrete IFN-γ or not. This suggests that apoptosis results from paracrine signalling (e.g. from one T cell to another) rather than autocrine signalling. Moreover, our data suggest that IFN-γ-mediated T cell loss is unlikely to occur solely via the classical intrinsic pathway of apoptosis since T cell expression of the pro-apoptotic molecules BIM, BAD and BAX did not differ significantly between WT and IFN-$\gamma^{-/-}$ mice. One possibility is that IFN-γ upregulates TNF production and, consequently, that apoptosis is indirectly induced in WT mice by increased death receptor signalling (Trail, TNFR1, DR4/5). Importantly, as the expression of CTLA-4 and PD-1 on splenic $CD4^+$ and $CD8^+$ T cells was unaltered in IFN-$\gamma^{-/-}$ mice during infection, it is unlikely that these pathways play a large role in regulating the survival and contraction phases of the splenic T cell response during *P. berghei* ANKA infection. Moreover, attenuated expression of CTLA-4 and PD-1 by tissue-accumulating $CD4^+$ T cells did not enhance their accumulation within non-lymphoid tissues in IFN-$\gamma^{-/-}$ mice, also suggesting that cell-intrinsic expression of these co-stimulatory molecules does not significantly regulate $CD4^+$ T cell migration into non-lymphoid tissues during *P. berghei* ANKA infection. Nevertheless, we cannot exclude the possibility that reduced CTLA-4 expression contributed to enhanced $CD8^+$ T cell survival within the lungs of IFN-$\gamma^{-/-}$ mice. The role of CTLA-4 in controlling CD8+ T cell survival and accumulation of CD8+ T cells within the brain is unclear, as although CTLA-4 expression by brain infiltrating CD8+ T cells was lower in IFN-$\gamma^{-/-}$ mice, accumulation of cells was also attenuated.

In summary, we have demonstrated heterogeneous and tissue specific control of $CD4^+$ and $CD8^+$ T cell responses by IFN-γ during *P. berghei* ANKA infection. Overall, splenic T cell responses appeared stronger in IFN-$\gamma^{-/-}$ mice, due primarily to reduced T cell apoptosis. Importantly, during *P. berghei* ANKA infection, IFN-γ appears to have very different effects on activation and migration of $CD4^+$ and $CD8^+$ T cells in tissues such lung and brain and this is not directly related to the cell-intrinsic expression level of IFN-γR. Thus, altered accumulation of $CD8^+$ T cells within the lung, liver and brain in WT and IFN-$\gamma^{-/-}$ mice during *P. berghei* ANKA infection is likely due to multiple factors, including reduced apoptosis within the spleen and tissues in IFN-$\gamma^{-/-}$ mice combined with altered tissue-specific signals regulating cellular adhesion and chemotaxis. These observations increase our understanding of the role of IFN-γ in the pathogenesis of ECM and may have relevance for understanding the role of IFN-γ in the pathogenesis of human CM.

Supplementary Material

Refer to Web version on PubMed Central for supplementary material.

References

1. de Souza JB, Hafalla JC, Riley EM, Couper KN. Cerebral malaria: why experimental murine models are required to understand the pathogenesis of disease. Parasitology. 2010; 137:755–772. [PubMed: 20028608]
2. Riley EM, Couper KN, Helmby H, Hafalla JC, de Souza JB, Langhorne J, Jarra WB, Zavala F. Neuropathogenesis of human and murine malaria. Trends Parasitol. 2010; 26:277–278. [PubMed: 20338809]
3. Amani V, Vigario AM, Belnoue E, Marussig M, Fonseca L, Mazier D, Renia L. Involvement of IFN-gamma receptor-medicated signaling in pathology and anti-malarial immunity induced by Plasmodium berghei infection. Eur J Immunol. 2000; 30:1646–1655. [PubMed: 10898501]
4. Belnoue E, Potter SM, Rosa DS, Mauduit M, Gruner AC, Kayibanda M, Mitchell AJ, Hunt NH, Renia L. Control of pathogenic CD8+ T cell migration to the brain by IFN-gamma during experimental cerebral malaria. Parasite Immunol. 2008; 30:544–553. [PubMed: 18665903]
5. Grau GE, Heremans H, Piguet PF, Pointaire P, Lambert PH, Billiau A, Vassalli P. Monoclonal antibody against interferon gamma can prevent experimental cerebral malaria and its associated overproduction of tumor necrosis factor. Proc Natl Acad Sci U S A. 1989; 86:5572–5574. [PubMed: 2501793]
6. Hunt NH, Golenser J, Chan-Ling T, Parekh S, Rae C, Potter S, Medana IM, Miu J, Ball HJ. Immunopathogenesis of cerebral malaria. Int J Parasitol. 2006; 36:569–582. [PubMed: 16678181]
7. Van den Steen PE, Deroost K, Van Aelst I, Geurts N, Martens E, Struyf S, Nie CQ, Hansen DS, Matthys P, Van Damme J, Opdenakker G. CXCR3 determines strain susceptibility to murine cerebral malaria by mediating T lymphocyte migration toward IFN-gamma-induced chemokines. Eur J Immunol. 2008; 38:1082–1095. [PubMed: 18383042]
8. Lundie RJ, de Koning-Ward TF, Davey GM, Nie CQ, Hansen DS, Lau LS, Mintern JD, Belz GT, Schofield L, Carbone FR, Villadangos JA, Crabb BS, Heath WR. Blood-stage Plasmodium infection induces CD8+ T lymphocytes to parasite-expressed antigens, largely regulated by CD8alpha+ dendritic cells. Proc Natl Acad Sci U S A. 2008; 105:14509–14514. [PubMed: 18799734]
9. Miyakoda M, Kimura D, Yuda M, Chinzei Y, Shibata Y, Honma K, Yui K. Malaria-specific and nonspecific activation of CD8+ T cells during blood stage of Plasmodium berghei infection. J Immunol. 2008; 181:1420–1428. [PubMed: 18606696]
10. deWalick S, Amante FH, McSweeney KA, Randall LM, Stanley AC, Haque A, Kuns RD, MacDonald KP, Hill GR, Engwerda CR. Cutting edge: conventional dendritic cells are the critical APC required for the induction of experimental cerebral malaria. J Immunol. 2007; 178:6033–6037. [PubMed: 17475826]

Europe PMC Funders Author Manuscripts

11. Campanella GS, Tager AM, El Khoury JK, Thomas SY, Abrazinski TA, Manice LA, Colvin RA, Luster AD. Chemokine receptor CXCR3 and its ligands CXCL9 and CXCL10 are required for the development of murine cerebral malaria. Proc Natl Acad Sci U S A. 2008; 105:4814–4819. [PubMed: 18347328]
12. Miu J, Mitchell AJ, Muller M, Carter SL, Manders PM, McQuillan JA, Saunders BM, Ball HJ, Lu B, Campbell IL, Hunt NH. Chemokine gene expression during fatal murine cerebral malaria and protection due to CXCR3 deficiency. J Immunol. 2008; 180:1217–1230. [PubMed: 18178862]
13. Hansen DS, Bernard NJ, Nie CQ, Schofield L. NK cells stimulate recruitment of CXCR3+ T cells to the brain during Plasmodium berghei-mediated cerebral malaria. J Immunol. 2007; 178:5779–5788. [PubMed: 17442962]
14. Renia L, Potter SM, Mauduit M, Rosa DS, Kayibanda M, Deschemin JC, Snounou G, Gruner AC. Pathogenic T cells in cerebral malaria. Int J Parasitol. 2006; 36:547–554. [PubMed: 16600241]
15. Haque A, Best SE, Unosson K, Amante FH, de Labastida F, Anstey NM, Karupiah G, Smyth MJ, Heath WR, Engwerda CR. Granzyme B Expression by CD8+ T Cells Is Required for the Development of Experimental Cerebral Malaria. J Immunol. 2011; 186:6148–6156. [PubMed: 21525386]
16. Amante FH, Haque A, Stanley AC, Fde L. Rivera, Randall LM, Wilson YA, Yeo G, Pieper C, Crabb BS, de Koning-Ward TF, Lundie RJ, Good MF, Pinzon-Charry A, Pearson MS, Duke MG, McManus DP, Loukas A, Hill GR, Engwerda CR. Immune-mediated mechanisms of parasite tissue sequestration during experimental cerebral malaria. J Immunol. 2010; 185:3632–3642. [PubMed: 20720206]
17. Claser C, Malleret B, Gun SY, Wong AY, Chang ZW, Teo P, See PC, Howland SW, Ginhoux F, Renia L. CD8+ T cells and IFN-gamma mediate the time-dependent accumulation of infected red blood cells in deep organs during experimental cerebral malaria. PLoS One. 2011; 6:e18720. [PubMed: 21494565]
18. Potter S, Chan-Ling T, Ball HJ, Mansour H, Mitchell A, Maluish L, Hunt NH. Perforin mediated apoptosis of cerebral microvascular endothelial cells during experimental cerebral malaria. Int J Parasitol. 2006; 36:485–496. [PubMed: 16500656]
19. Afkarian M, Sedy JR, Yang J, Jacobson NG, Cereb N, Yang SY, Murphy TL, Murphy KM. T-bet is a STAT1-induced regulator of IL-12R expression in naive CD4+ T cells. Nat Immunol. 2002; 3:549–557. [PubMed: 12006974]
20. Schulz EG, Mariani L, Radbruch A, Hofer T. Sequential polarization and imprinting of type 1 T helper lymphocytes by interferon-gamma and interleukin-12. Immunity. 2009; 30:673–683. [PubMed: 19409816]
21. Zhang Y, Apilado R, Coleman J, Ben-Sasson S, Tsang S, Hu-Li J, Paul WE, Huang H. Interferon gamma stabilizes the T helper cell type 1 phenotype. J Exp Med. 2001; 194:165–172. [PubMed: 11457891]
22. Aloisi F, Ria F, Penna G, Adorini L. Microglia are more efficient than astrocytes in antigen processing and in Th1 but not Th2 cell activation. J Immunol. 1998; 160:4671–4680. [PubMed: 9590212]
23. Whitmire JK, Benning N, Whitton JL. Cutting edge: early IFN-gamma signaling directly enhances primary antiviral CD4+ T cell responses. J Immunol. 2005; 175:5624–5628. [PubMed: 16237051]
24. Whitmire JK, Tan JT, Whitton JL. Interferon-gamma acts directly on CD8+ T cells to increase their abundance during virus infection. J Exp Med. 2005; 201:1053–1059. [PubMed: 15809350]
25. Mayer KD, Mohrs K, Reiley W, Wittmer S, Kohlmeier JE, Pearl JE, Cooper AM, Johnson LL, Woodland DL, Mohrs M. Cutting edge: T-bet and IL-27R are critical for in vivo IFN-gamma production by CD8 T cells during infection. J Immunol. 2008; 180:693–697. [PubMed: 18178806]
26. Badovinac VP, Tvinnereim AR, Harty JT. Regulation of antigen-specific CD8+ T cell homeostasis by perforin and interferon-gamma. Science. 2000; 290:1354–1358. [PubMed: 11082062]
27. Dalton DK, Haynes L, Chu CQ, Swain SL, Wittmer S. Interferon gamma eliminates responding CD4 T cells during mycobacterial infection by inducing apoptosis of activated CD4 T cells. J Exp Med. 2000; 192:117–122. [PubMed: 10880532]
28. Li X, McKinstry KK, Swain SL, Dalton DK. IFN-gamma acts directly on activated CD4+ T cells during mycobacterial infection to promote apoptosis by inducing components of the intracellular

apoptosis machinery and by inducing extracellular proapoptotic signals. J Immunol. 2007; 179:939–949. [PubMed: 17617585]

29. Florido M, Pearl JE, Solache A, Borges M, Haynes L, Cooper AM, Appelberg R. Gamma interferon-induced T-cell loss in virulent Mycobacterium avium infection. Infect Immun. 2005; 73:3577–3586. [PubMed: 15908387]
30. Turner SJ, Olivas E, Gutierrez A, Diaz G, Doherty PC. Disregulated influenza A virus-specific CD8+ T cell homeostasis in the absence of IFN-gamma signaling. J Immunol. 2007; 178:7616–7622. [PubMed: 17548597]
31. Xu H, Wipasa J, Yan H, Zeng M, Makobongo MO, Finkelman FD, Kelso A, Good MF. The mechanism and significance of deletion of parasite-specific CD4(+) T cells in malaria infection. J Exp Med. 2002; 195:881–892. [PubMed: 11927632]
32. Refaeli Y, Van Parijs L, Alexander SI, Abbas AK. Interferon gamma is required for activation-induced death of T lymphocytes. J Exp Med. 2002; 196:999–1005. [PubMed: 12370261]
33. Foulds KE, Rotte MJ, Paley MA, Singh B, Douek DC, Hill BJ, O'Shea JJ, Watford WT, Seder RA, Wu CY. IFN-gamma mediates the death of Th1 cells in a paracrine manner. J Immunol. 2008; 180:842–849. [PubMed: 18178823]
34. Russell MS, Dudani R, Krishnan L, Sad S. IFN-gamma expressed by T cells regulates the persistence of antigen presentation by limiting the survival of dendritic cells. J Immunol. 2009; 183:7710–7718. [PubMed: 19923462]
35. Wipasa J, Xu H, Stowers A, Good MF. Apoptotic deletion of Th cells specific for the 19-kDa carboxyl-terminal fragment of merozoite surface protein 1 during malaria infection. J Immunol. 2001; 167:3903–3909. [PubMed: 11564808]
36. Sanchez-Torres L, Rodriguez-Ropon A, Aguilar-Medina M, Favila-Castillo L. Mouse splenic CD4+ and CD8+ T cells undergo extensive apoptosis during a Plasmodium chabaudi chabaudi AS infection. Parasite Immunol. 2001; 23:617–626. [PubMed: 11737664]
37. Mukherjee P, Devi YS, Chauhan VS. Blood stage malaria antigens induce different activation-induced cell death programs in splenic CD4+T cells. Parasite Immunol. 2008; 30:497–514. [PubMed: 18643960]
38. Good MF, Xu H, Wykes M, Engwerda CR. Development and regulation of cell-mediated immune responses to the blood stages of malaria: implications for vaccine research. Annu Rev Immunol. 2005; 23:69–99. [PubMed: 15771566]
39. Villarino AV, Gallo E, Abbas AK. STAT1-activating cytokines limit Th17 responses through both T-bet-dependent and -independent mechanisms. J Immunol. 2010; 185:6461–6471. [PubMed: 20974984]
40. Paludan SR. Interleukin-4 and interferon-gamma: the quintessence of a mutual antagonistic relationship. Scand J Immunol. 1998; 48:459–468. [PubMed: 9822252]
41. Schroder K, Hertzog PJ, Ravasi T, Hume DA. Interferon-gamma: an overview of signals, mechanisms and functions. J Leukoc Biol. 2004; 75:163–189. [PubMed: 14525967]
42. Monso-Hinard C, Lou JN, Behr C, Juillard P, Grau GE. Expression of major histocompatibility complex antigens on mouse brain microvascular endothelial cells in relation to susceptibility to cerebral malaria. Immunology. 1997; 92:53–59. [PubMed: 9370924]
43. Nie CQ, Bernard NJ, Norman MU, Amante FH, Lundie RJ, Crabb BS, Heath WR, Engwerda CR, Hickey MJ, Schofield L, Hansen DS. IP-10-mediated T cell homing promotes cerebral inflammation over splenic immunity to malaria infection. PLoS Pathog. 2009; 5:e1000369. [PubMed: 19343215]

Europe PMC Funders Author Manuscripts

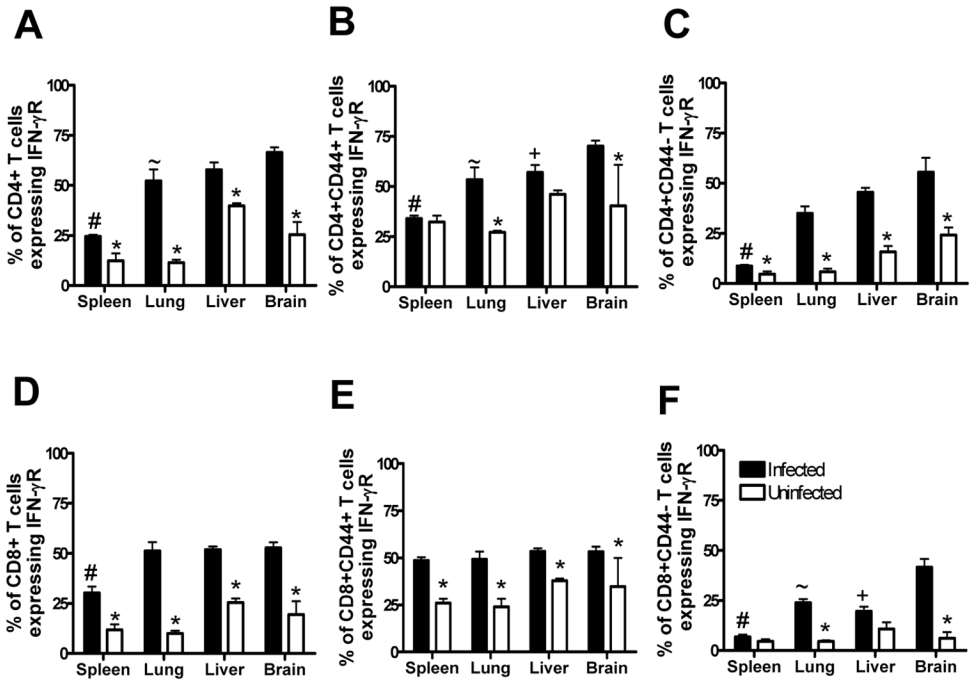

Figure 1. IFN-γR expression on T cell populations in spleen, lung, liver and brain during the course of *P. berghei* ANKA infection

WT mice were infected i.v. with 10^4 *P. berghei* ANKA pRBC. On day 7 post-infection the surface expression of IFN-γR on naïve ($CD44^-$) and activated ($CD44^+$) CD4+ and $CD8^+$ T cells was determined by flow cytometry. (A-F) The expression of IFN-γR on (A-C) $CD4^+$ T cells and (D-F) $CD8^+$ T cells isolated from naïve or infected WT mice. (A, D) The frequency of total $CD4^+$ and $CD8^+$ T cells expressing IFN-γR. (B, E) The frequency of activated ($CD44^+$) $CD4^+$ and $CD8^+$ T cells expressing IFN-γR. (C, F) The frequency of naive ($CD44^-$) $CD4^+$ and $CD8^+$ T cells expressing IFN-γR. The results are the mean +/− SEM of the group with 4-5 mice per group. The results are representative of 2 separate experiments. * $P<0.05$ infected vs uninfected; # $P<0.05$ spleen infected versus lung, liver, brain infected; ~ $P<0.05$ lung infected vs brain infected; + $P<0.05$ liver infected vs brain infected.

Europe PMC Funders Author Manuscripts

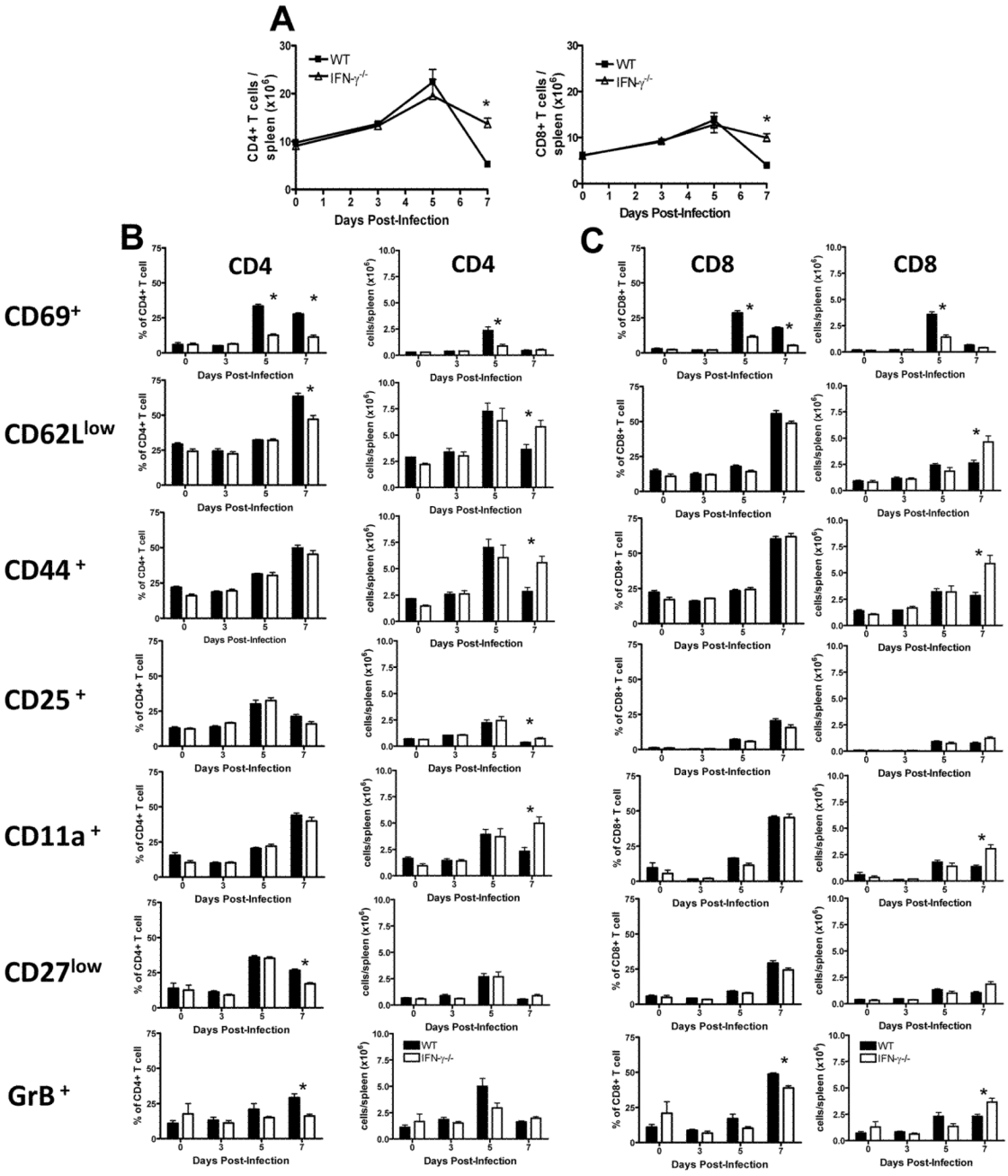

Figure 2. IFN-γ is not required for activation of splenic CD4$^+$ or CD8$^+$ T cells during *P. berghei* ANKA infection

WT and IFN-γ$^{-/-}$ mice were infected i.v. with 10^4 *P. berghei* ANKA pRBC. (A) Total numbers of splenic CD4$^+$ and CD8$^+$ T cells were determined by flow cytometry. (B, C) The frequency (left columns) and total number (right columns) of activated (B) CD4$^+$ and (C) CD8$^+$ T cells within the spleen was determined by flow cytometry. The results are the mean +/− SEM of the group with 3-5 mice per group. The results are representative of 3 separate experiments. * P<0.05 between WT and IFN-γ$^{-/-}$ mice

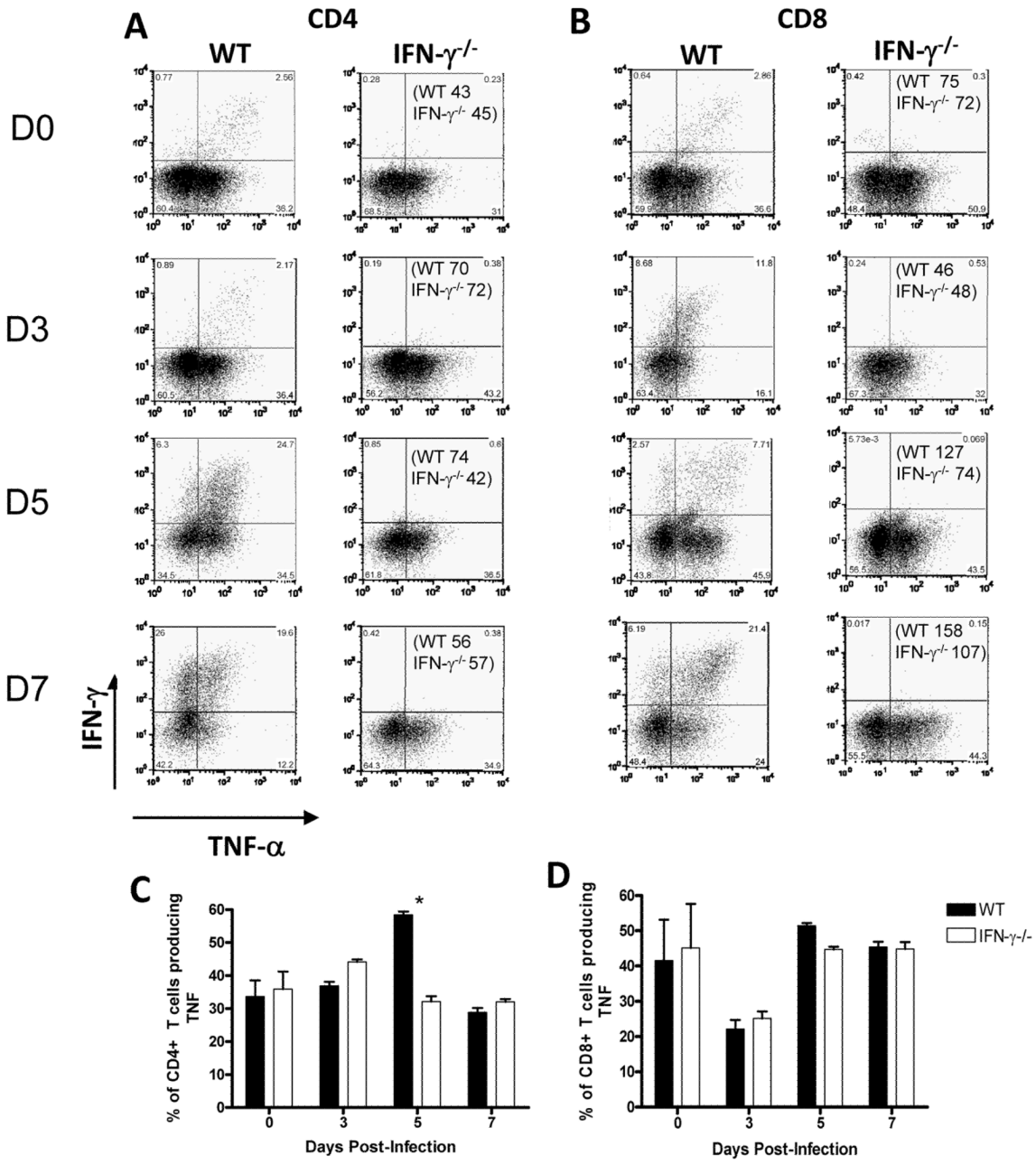

Figure 3. TNF production by T cells is slightly reduced in the absence of IFN-γ during *P. berghei* ANKA infection

WT and IFN-$\gamma^{-/-}$ mice were infected i.v. with 10^4 *P. berghei* ANKA pRBC. Intracellular production of TNF and IFN-γ by of naïve and infection-derived WT and IFN-$\gamma^{-/-}$ $CD4^+$ and $CD8^+$ T cells was assessed following *in vitro* stimulation of splenocytes with PMA and ionomycin, in the presence of Brefeldin A, for 5hrs. (A, B) representative dot plots showing the level of IFN-γ and TNF production in gated (A) $CD4^+$ and (B) $CD8^+$ T cells. Bracketed numbers within plots represent the MFI of TNF production for WT and IFN-$\gamma^{-/-}$ cells. (C, D) The frequencies of TNF^+ $CD4^+$ (C) and $CD8^+$ T cells (D). The results are the mean +/−

SEM of the group with 3-5 mice per group. The results are representative of 3 separate experiments. * $P<0.05$ between WT and IFN-$\gamma^{-/-}$ mice

Europe PMC Funders Author Manuscripts

Europe PMC Funders Author Manuscripts

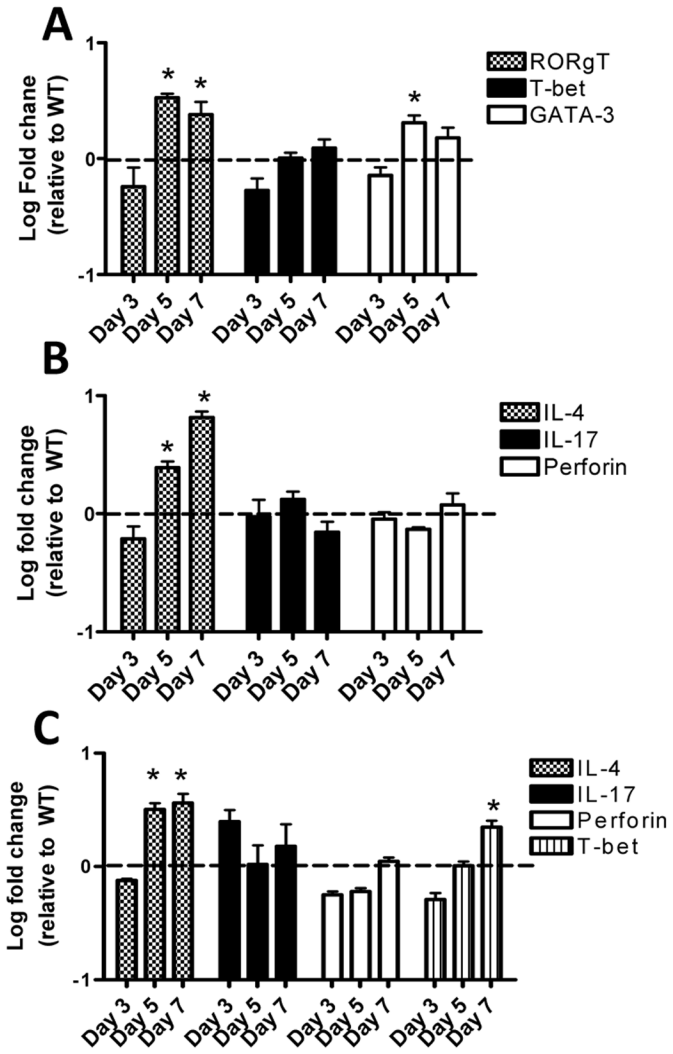

Figure 4. Minor modulation of T cell lineage commitment and expression of associated cytokines during malaria infection in the absence of IFN-γ

WT and IFN-$\gamma^{-/-}$ mice were infected i.v. with 10^4 *P. berghei* ANKA pRBC. (A, B) Splenic CD4+ and (C) CD8+ T cells were purified from *P. berghei* ANKA infected mice (day 3, 5 and 7) and the level of gene expression was determined by rtPCR. Results are expressed as the log fold change relative to the level in infection derived WT $CD4^+$ T cells. The results are representative of 2 separate experiments. * $P<0.05$ between WT and IFN-$\gamma^{-/-}$ mice.

Europe PMC Funders Author Manuscripts

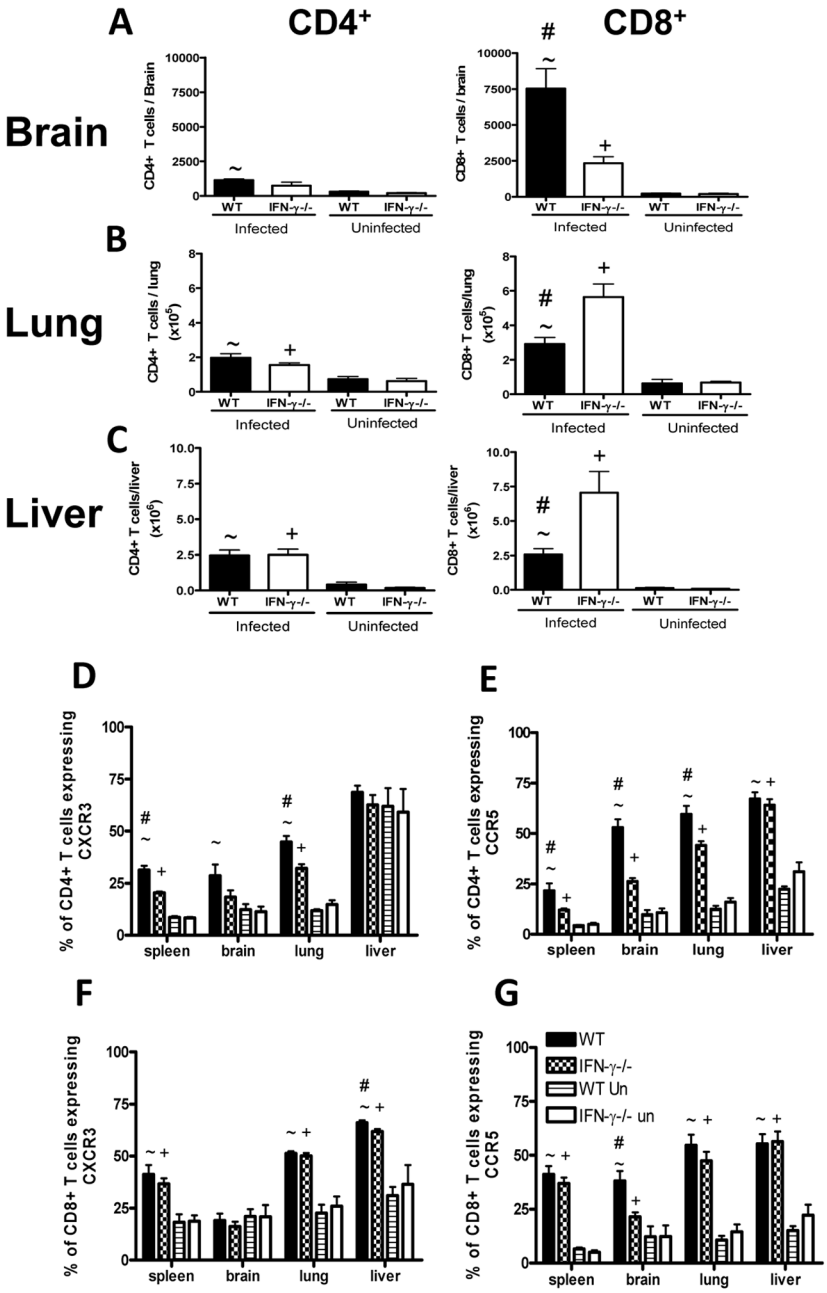

Figure 5. Altered patterns of T cell migration in IFN-$\gamma^{-/-}$ mice during *P. berghei* ANKA is not correlated with cell-intrinsic expression of CXCR3 and CCR5

WT and IFN-$\gamma^{-/-}$ mice were infected i.v. with 10^4 *P. berghei* ANKA pRBC. (A-C) The total numbers of $CD4^+$ and $CD8^+$ T cells in the (A) brain, (B) liver and (c) lung of WT and IFN-$\gamma^{-/-}$ mice on day 7 of infection. (D-G) The frequencies of (D, E) $CD4^+$ and (F, G) $CD8^+$ T cells expressing (D, F) CXCR3 and (E, G) CCR5 in the various organs on day 7 of infection. The results are the mean +/− SEM of the group with 3-5 mice per group. The results are representative of 4 separate experiments. # $P<0.05$ between infected WT and IFN-$\gamma^{-/-}$ mice; ~ $P<0.05$ between infected WT and uninfected WT mice; + $P<0.05$ between infected IFN-$\gamma^{-/-}$ and uninfected IFN-$\gamma^{-/-}$ mice.

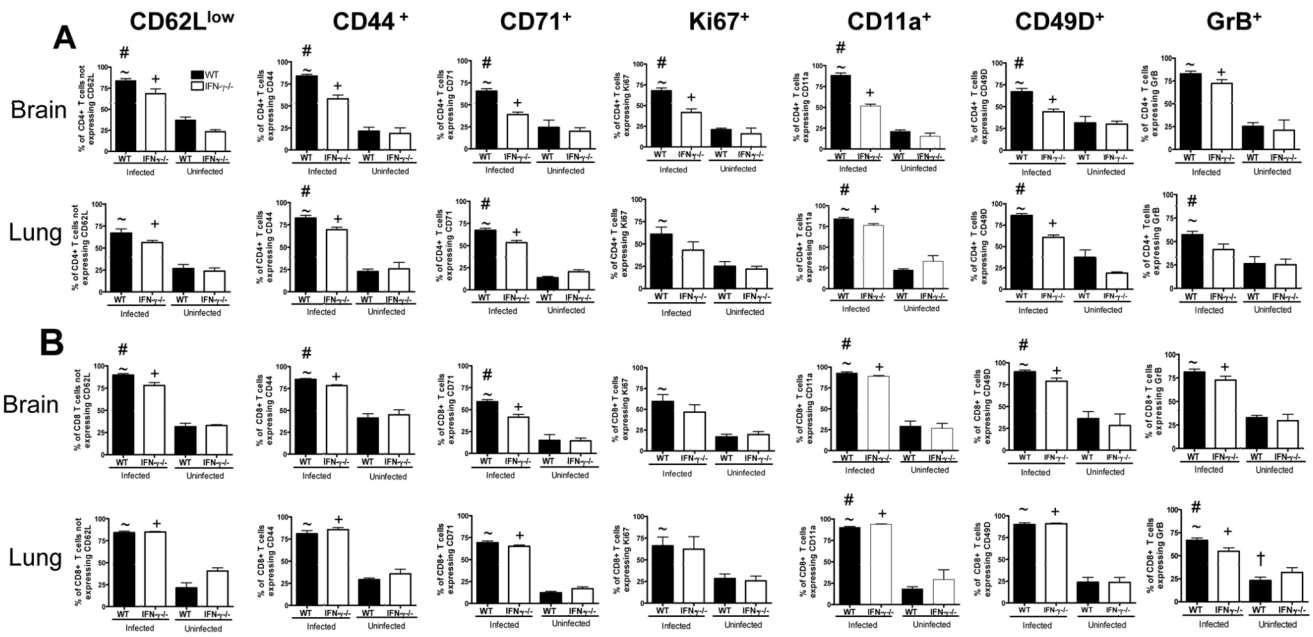

Figure 6. Heterogeneous control of effector T cell responses by IFN-γ within peripheral tissues during *P. berghei* ANKA infection

WT and IFN-$\gamma^{-/-}$ mice were infected i.v. with 10^4 *P. berghei* ANKA pRBC. The frequencies of (A) $CD4^+$ and (B) $CD8^+$ T cells expressing various markers of activation and function in the brain and lung of WT and IFN-$\gamma^{-/-}$ mice on day 7 of infection. The results are the mean +/− SEM of the group with 3-5 mice per group. The results are representative of 4 separate experiments. # $P<0.05$ between infected WT and IFN-$\gamma^{-/-}$ mice; † $P<0.05$ between uninfected WT and IFN-$\gamma^{-/-}$ mice; ~ $P<0.05$ between infected WT and uninfected WT mice; + $P<0.05$ between infected IFN-$\gamma^{-/-}$ and uninfected IFN-$\gamma^{-/-}$ mice.

Europe PMC Funders Author Manuscripts

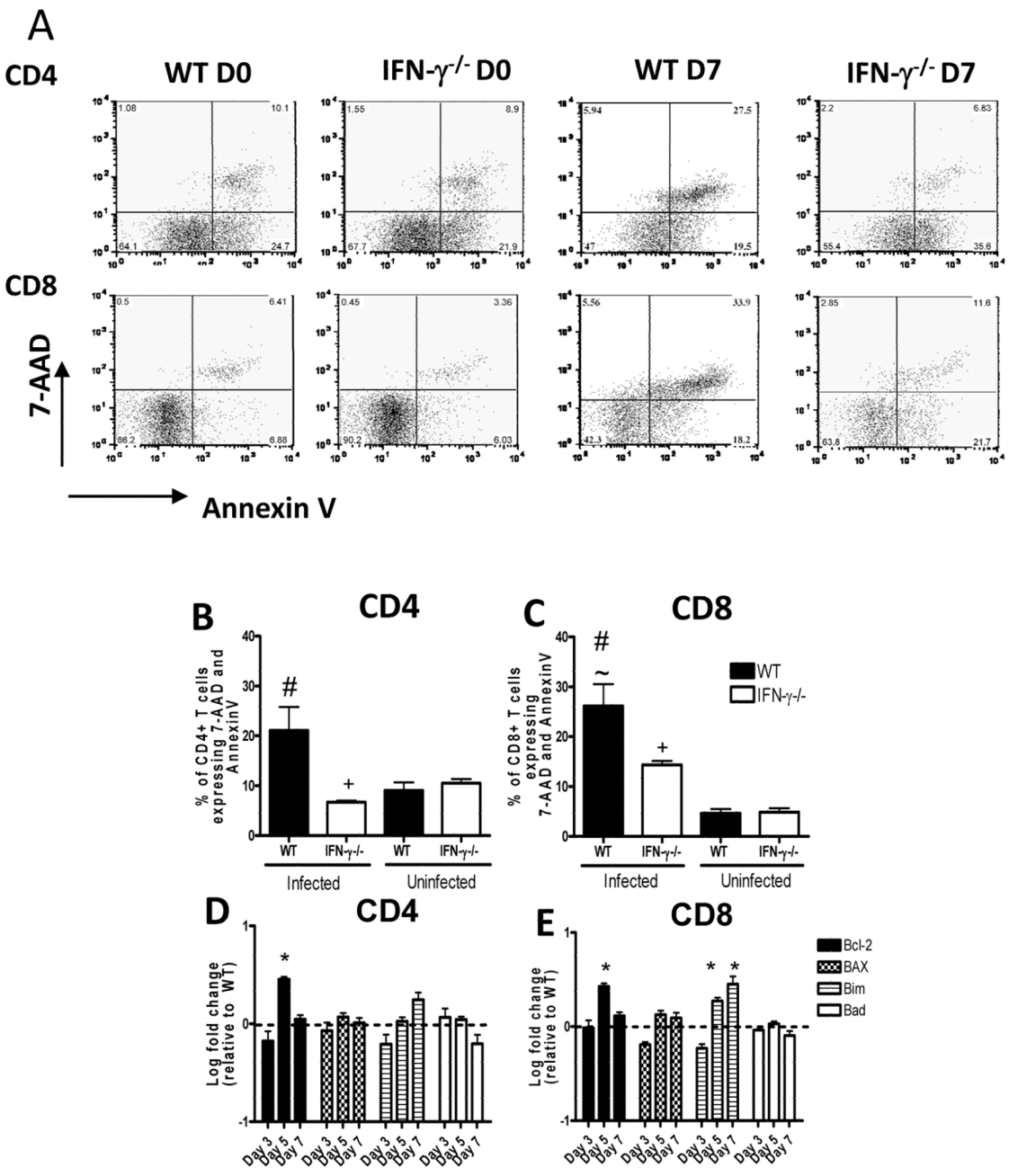

Figure 7. IFN-γ promotes apoptosis of splenic T cells during *P. berghei* ANKA infection

WT and IFN-$\gamma^{-/-}$ mice were infected i.v. with 10^4 *P. berghei* ANKA pRBC. (A) Representative dot plots showing the surface expression of Annexin V and 7-AAD on naive and infection-derived (D7) $CD4^+$ and $CD8^+$ T cells. (B, C) The frequencies of late stage apoptotic (7-AAD^+, Annexin-V^+) $CD4^+$ T cells (B) and $CD8^+$ T cells (C) in the spleen of naive and infected (Day 7) WT and IFN-$\gamma^{-/-}$ mice. (D, E) The expression of pro- and anti-apoptotic regulators in purified WT and IFN-$\gamma^{-/-}$ $CD4^+$ (D) and $CD8^+$ (E) T cells on various days of infection. (B-E) The results are the mean +/− SEM of the group with 3-5 mice per group. (D, E) Results are expressed as the log fold change relative to the level in infection derived WT $CD4^+$ T cells. The results are representative of 4 separate experiments.

(B, C) # P<0.05 between infected WT and IFN-$\gamma^{-/-}$ mice; ~ P<0.05 between infected WT and uninfected WT mice; + P<0.05 between infected IFN-$\gamma^{-/-}$ and uninfected IFN-$\gamma^{-/-}$ mice. (D, E) * P<0.05 between WT and IFN-$\gamma^{-/-}$ mice.

Europe PMC Funders Author Manuscripts

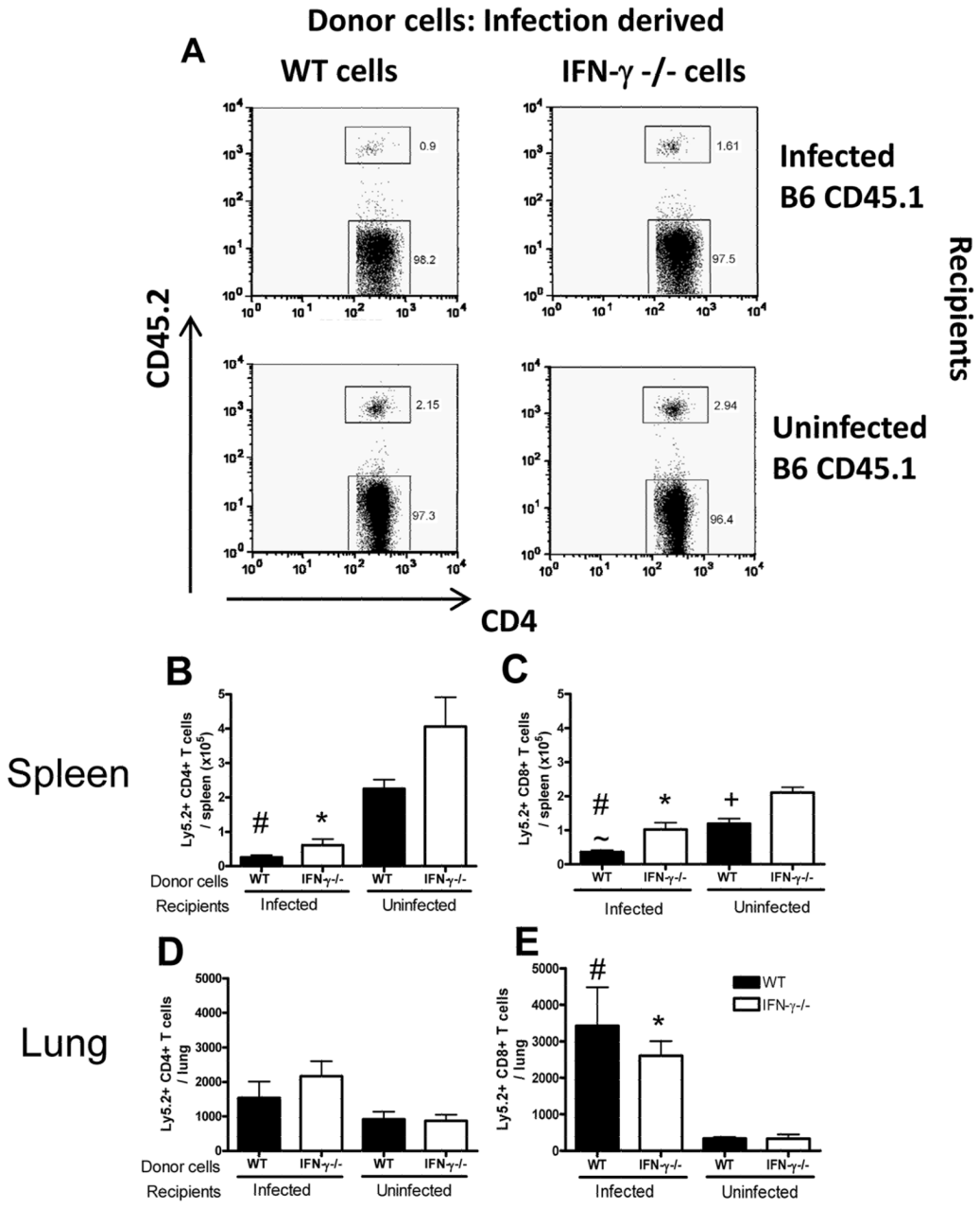

Figure 8. WT and IFN-$\gamma^{-/-}$ infection-derived T cells behave similarly in an IFN-γ sufficient environment

WT and IFN-$\gamma^{-/-}$ mice (both CD45.2$^+$) were infected i.v. with 10^4 *P. berghei* ANKA pRBC. On day 5 post-infection splenic CD4$^+$ and CD8$^+$ T cells were purified and transferred i.v. into naïve or *P. berghei* ANKA infected (Day 5) C57BL/6 Ly5.1$^+$ mice. (A) Representative dot plots showing the recovery of adoptively transferred WT or IFN-$\gamma^{-/-}$ CD45.2$^+$ CD4$^+$ T cells from the spleen, 2 days post-transfer. (B-E) The numbers of adoptively transferred (B, D) CD4$^+$ CD45.2$^+$ and (C, E) CD8$^+$ CD45.2$^+$ T cells in (B, C) spleen and (D, E) lung, in uninfected and infected mice. The results are the mean +/− SEM of the group with 3-4 mice per group. The results are representative of 2 separate

experiments. # P<0.05 between infected recipients of WT cells vs uninfected recipients of WT cells; * P<0.05 between infected recipients of IFN-$\gamma^{-/-}$ cells vs uninfected recipients of IFN-$\gamma^{-/-}$ cells; ~ P<0.05 between infected recipients of WT cells vs infected recipients of IFN-$\gamma^{-/-}$ cells; + P<0.05 between uninfected recipients of WT cells vs uninfected recipients of IFN-$\gamma^{-/-}$ cells

Europe PMC Funders Author Manuscripts

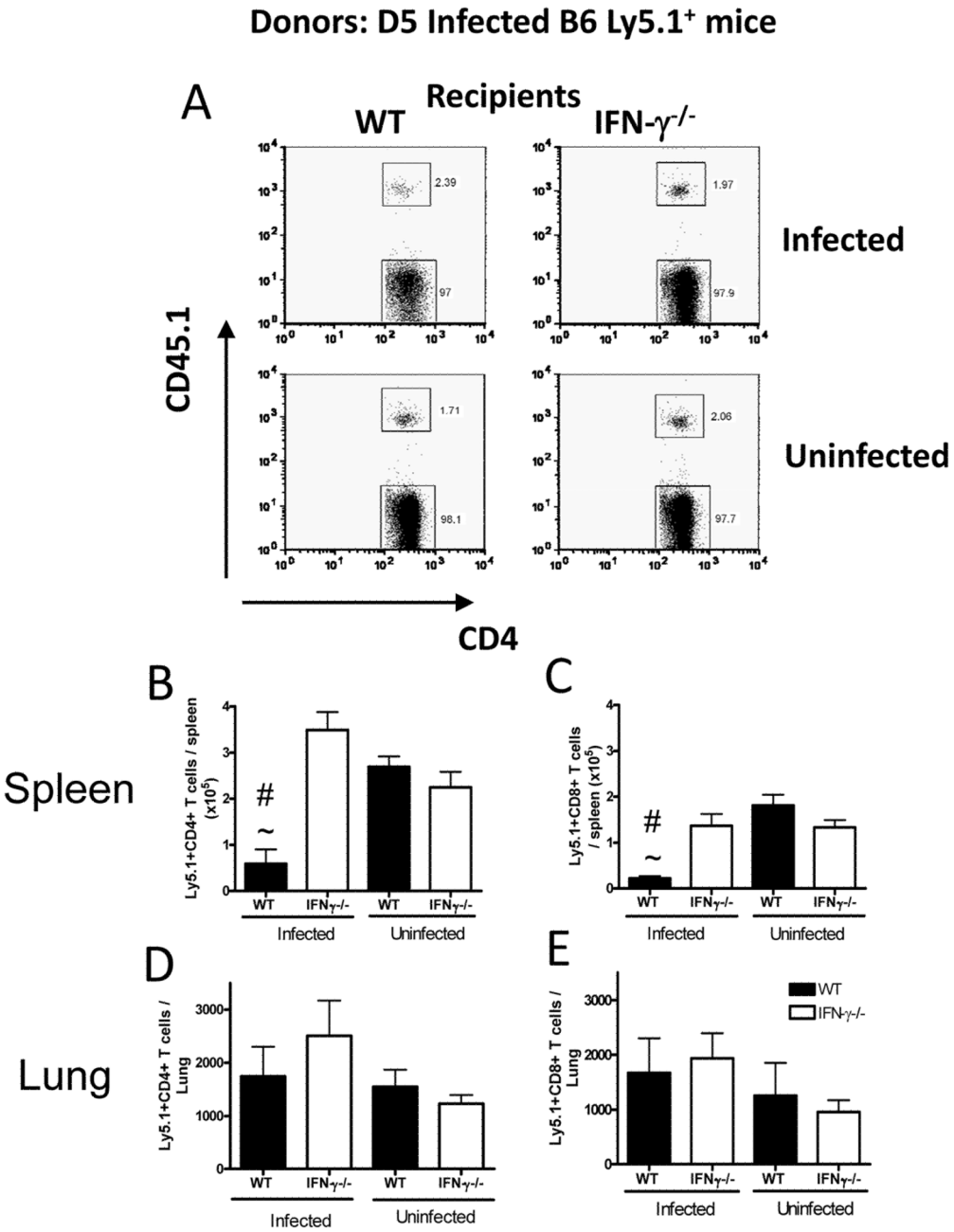

Figure 9. Environmental rather than cell-intrinsic signals primarily determine the maintenance of splenic of T cells during *P. berghei* ANKA infection

C57BL/6 Ly5.1$^+$ mice were infected i.v. with 10^4 *P. berghei* ANKA pRBC. On day 5 post-infection, splenic CD4$^+$ and CD8$^+$ T cells were purified and transferred into naïve or *P. berghei* ANKA infected (day 5) WT or IFN-$\gamma^{-/-}$ (both Ly5.2$^+$) mice. (A) Representative dot plots showing the recovery of adoptively transferred CD45.1$^+$ CD4$^+$ T cells, 2 days post-transfer. (B-E) The numbers of adoptively transferred (B, D) CD4$^+$ CD45.1$^+$ and (C, E) CD8+ CD45.1$^+$ T cells in (B, C) spleen and (D, E) lung, in uninfected and infected mice. The results are the mean +/− SEM of the group with 3-4 mice per group. The results are

representative of 2 separate experiments. # P<0.05 between infected WT and IFN-$\gamma^{-/-}$ mice; ~ P<0.05 between infected WT and uninfected WT mice.

Europe PMC Funders Author Manuscripts